SEPTEMBER 1980 PPPL-1686
UC 20g

Dr. 1740

CONF-800768--1

STARK BROADENING OF ISOLATED LINES FROM HIGH-Z EMITTERS IN DENSE PLASMAS

BY

J. C. WEISHEIT AND E. L. POLLOCK

PLASMA PHYSICS LABORATORY

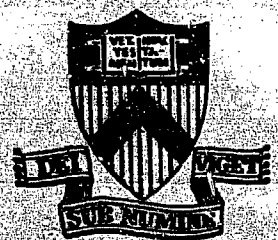

PRINCETON UNIVERSITY
PRINCETON, NEW JERSEY

DISTRIBUTION OF THIS DOCUMENT IS UNLIMITED

This work was supported by the U.S. Department of Energy Contract No. DE-AC02-76-CHO 3073. Reproduction, translation, publication, use and disposal, in whole or in part, by or for the United States government is permitted.

NOTICE

Printed in the United States of America.

Available from:

National Technical Information Service
U. S. Department of Commerce
5285 Port Royal Road
Springfield, Virginia 22151

Price: Printed Copy $ * ; Microfiche $3.00

*Pages	NTIS Selling Price
1-50	$4.00
51-150	$5.45
151-325	$7.60
326-500	$10.60
501-1000	$13.60

STARK BROADENING OF ISOLATED LINES FROM HIGH-Z EMITTERS IN DENSE PLASMAS

J. C. Weisheit

Plasma Physics Laboratory, Princeton University

P.O. Box 451, Princeton, N.J. 08544 USA

E. L. Pollock

Theoretical Physics Division, Lawrence Livermore Laboratory

P.O. Box 808, Livermore, CA 94550 USA

ABSTRACT

The joint distribution of the electric microfield and its longitudinal derivative is required for the calculation of line profiles for the He-like ions in very dense plasmas. We used a molecular dynamics code to compute "exact" distributions in single- and multi-component plasmas, and then we investigated various analytical approximations to these results. We found that a simplified, two-nearest-neighbor scheme leads to suprisingly accurate distribution functions. Our results are illustrated by sample profiles for Ne^{+8} and Ar^{+16} resonance lines.

1. Introduction

X-ray line shapes are useful diagnostics of conditions in the very dense plasmas ($N_e > 10^{22}$ cm^{-3}) now being generated by inertial confinement experiments [1], and also they are needed to determine the performance of short-wavelength laser schemes [2]. Even though the helium-like ions of heavy elements usually are prevalent under a much greater range of plasma temperatures than are the hydrogenic ions, most attention has been paid to the simpler, one-electron spectra. An interesting aspect of the broadening of the He-like ion lines is that the (quasi-static) quadratic-Stark and quadrupolar perturbations, which vary as the square of the plasma microfield $\vec{F} = F\hat{\xi}$ and its longitudinal derivative $G = -(1/2)\,\hat{\xi} \cdot (\partial\vec{F}/\partial\xi)$, can be of comparable magnitude in the dense plasma regime. Moreover, unless the nearest neighbor (1NN) approximation is valid, these two broadening mechanisms are not completely correlated at all values of F.

We used a molecular dynamics code to compute the "exact" distributions of F and G in model plasmas of classical ions and electrons. Various approximations to these results were examined. The calculated distributions then were used to obtain sample profiles of two-electron neon and argon ions in dense plasmas. Relevant line broadening formulae are reviewed in Section 2; the molecular dynamics calculations are described in Section 3; and some computed line shapes are presented and discussed in Section 4.

2. Broadening Formulae for Isolated Lines of He-Like Ions

Let $h\nu_{ij}^{(o)} = E_i^{(o)} - E_j^{(o)}$ be the transition energy, in vacuo, of the spectral line due to the radiative decay from state $|i\rangle = |nSLJM\rangle$ to state $|j\rangle = |\tilde{n}SLJM\rangle$ in a two-electron ion of net charge Z_r. The probability that various perturbations of the radiator result in a photon whose energy lies

between $h\nu_{ij}^{(o)}$ and $h\nu_{ij}^{(o)} + \Delta E$ is defined to be $\phi\ (\Delta E)d(\Delta E)$. Electron impacts shift the line by an amount d and, together with random ion motions, produce a Voigt profile

$$\phi_v(\Delta E) = (1/\sqrt{\pi}\delta_D)\ H[(\Delta E - d)/\delta_D, a\ ]\ , \qquad (1)$$

where $\sqrt{\ln 2}\delta_D$ is the Doppler half-width at half-maximum incensity (HWHM), $a = \delta_e/\delta_D$ is the ratio of the electron impact HWHM to δ_D, and H is the Voigt function [3].

The Voigt profile neglects quasi-static ion broadening that, in dense plasmas, can be comparable to the electron-impact and Doppler mechanisms. Consider a helium-like ion radiating in the presence of a single stationary perturber of charge Z_p. (This is the nearest neighbor, or 1NN, approximation.) A multipole expansion of the electrostatic interaction between the active electron at $\vec{r}$ and the perturbing ion at $\vec{R} > \vec{r}$,

$$U = \Sigma_\lambda U_\lambda = -\ (Z_p e^2/R)\ \Sigma_\lambda (r/R)^\lambda P_\lambda\ (\vec{R}\ .\ \vec{r}/Rr)\ , \qquad (2)$$

leads to the first and second order eigenvalue corrections

$$E_i^{(1)} = \langle i|U_2|i\rangle\ , \qquad (3)$$

$$E_i^{(2)} = \Sigma_{k\neq i}\ \langle i|U_1|k\rangle\ \langle k|U_1|i\rangle/(E_i - E_k)\ . \qquad (4)$$

These matrix elements can be evaluated straight forwardly in the coupled $|nSLJM\rangle$ representation by means of Racah algebra techniques. In most calculations, the summation in Eq. (4) can be restricted to those states with

$n_k = n_i$. If $\vec{R}$ is chosen as the axis of quantization, both level-shift formulae simplify further.

When the 1NN approximation is not valid, the interaction U must be extended to include other perturbing ions Z_i at $\vec{R}_i$. Altogether, these ions produce a net electric field

$$\vec{F} = F\hat{\xi} = -\Sigma_i \; Z_i \; e\vec{R}_i/R_i^{\,3} \tag{5}$$

at the origin. It can be shown that the first-order, or ion-quadrupolar, shift is proportional to the quantity

$$G = -\,(1/2)\;\hat{\xi}\quad(\partial\vec{F}/\partial\xi)\quad, \tag{6}$$

which henceforth we refer to as the longitudinal derivative of the field. In order to obtain a tractable expression for $E^{(2)}$ when there are many perturbers, it is customary [4] to average $E^{(2)}$ with respect to the projection quantum number M. Then, it follows that the second-order, or quadratic-Stark, shift is proportional to F^2. Upon collecting results, we write the quasi-static level shift as

$$E_i^{(1)} + E_i^{(2)} = c_3(nSLJM)G + c_4(nSLJ)F^2\quad, \tag{7}$$

where the Stark coefficients are

$$c_3(nSLJM) = (-1)^{1-M-S}\;(2J+1)\;(2L+1)\;(nL|r^2|nL) \tag{8}$$
$$\times \begin{pmatrix} L & 2 & L \\ 0 & 0 & 0 \end{pmatrix} \begin{pmatrix} J & 2 & J \\ -M & 0 & M \end{pmatrix} \begin{Bmatrix} J & 2 & J \\ L & S & L \end{Bmatrix},$$

$$c_4(nSLJ) = (1/3) \sum_{L'J'} \frac{(2J' + 1)\ \max\ (L,L')\ (nL|r|nL')^2}{|E^{(o)}(nSLJ) - E^{(o)}(nSL'J')|} \begin{Bmatrix} J & 1 & J' \\ L' & S & L \end{Bmatrix}^2 \quad . \qquad (9)$$

We neglect Stark broadening of the lower level, and therefore the quasi-static profile of the line is simply related to the joint distribution P(F,G) of the microfield strength F and its longitudinal derivative G:

$$\phi_{QS}\ (\Delta E = E_i^{(1)} + E_i^{(2)})\ d(\Delta E) = P(F,G)\ dF\ dG \quad . \qquad (10)$$

The complete profile is given by the convolution of ϕ_v and ϕ_{QS}.

3. Molecular Dynamics Calculations

Distributions of F and G have been computed for model plasmas of classical ions in a uniform, charge-neutralizing background that represents the electrons. Our results probably are insensitive to this treatment of the electrons, but this assumption can be verified by comparison with a more realistic dense plasma model that treats electrons as point particles. At present it is known that the uniform-electron-background model and the more realistic model yield essentially identical ionic radial distribution functions [5]. The molecular dynamics method was used in our computations, although the simpler Monte Carlo method would also suffice to determine the time-independent quantities of interest here. A periodic system with 100 ions in a central cell was adopted. The microfields were determined by the Ewald method (see, for example, Hansen, et al [6]), and the longitudinal derivatives

were calculated by summing over particles in the periodic cell around each radiating ion (Evjen method).

3.1 One-Component Plasmas

In the limit of low density and high temperature, the Holtsmark microfield distribution is valid for one-component plasmas. But, because correlations between ions are ignored, the Holtsmark distribution strongly overestimates the probability of large microfields in the dense plasmas of interest here. Moreover, even for this simple model, there is no calculable expression for the joint distribution P(F,G) (cf. Chandrasekhar and von Neumann [7]).

The nearest neighbor (1NN) approximation gives the correct microfield distribution at sufficiently high values of the field $F = Ze/R^2$, and requires as input just the two-particle, radial distribution function g (R) for the ions. In terms of g (R), the probability that the radiator's nearest neighbor is in a spherical shell of radii R and R + dR is

$$W(R)\, dR = 4\pi \bar{N} R^2\, g(R) \exp[-\eta(R)]\, dR, \tag{11}$$

where $\bar{N}$ is the mean number density of ions, and where

$$\eta(R) = 4\pi \bar{N} \int_0^R s^2\, g(s)\, ds \tag{12}$$

is the expected number of perturbers within a sphere of radius R centered at the radiating ion. The 1NN microfield distribution is directly related to W(R), viz.

$$P(F) = W(R)\, |dR/dF| \quad . \tag{13}$$

Only values of g (R) near the origin are needed to evaluate these expressions, since W(R) goes rapidly to zero at large R-values. Fortunately, in the small-R region, simple yet accurate formulae for the radial distribution function already are available from work on pyconuclear reaction rate enhancement in stars [8,9].

Figure 1 compares the total microfield distribution and that due to the nearest neighbor in the cell, for a range of values of the Coulomb parameter

$$\Gamma = (Ze)^2/R_0kT \ . \qquad (14)$$

Here, T is the plasma temperature, and R_0 is the ion-sphere radius, defined by the expression $4/3\pi R_0^3 \bar{N} = 1$. Low values of the field strength F, arising from a nearly symmetrical arrangement of perturbers, cannot be reproduced by considering a single perturbing ion, and so the 1NN results are negligible at low F. In all cases, the 1NN approximation overestimates the probability of field strengths $F \sim Ze/R_0^2$, and then, as expected, approaches the exact distribution at large F-values.

The inclusion of the second nearest neighbor (2NN approximation) is seen in Figure 1 to yield substantial improvement over the 1NN results, for $\Gamma \leq 2$; this regime includes the plasmas generated in most laser-fusion experiments. The calculation of the probability $W(R_1,R_2,\theta)$ that the nearest perturber is at a distance R_1 from the radiator and that the second nearest perturber, at R_2, with $\vec{R}_1 \cdot \vec{R}_2 = R_1R_2\cos\theta$, in general requires knowledge of the three-particle distribution function $g^{(3)}$ $(R_1,R_2,R_{12} = |\vec{R}_2 - \vec{R}_1|)$, for which there is no simple expression. However, in the superposition approximation, $g^{(3)}$ is replaced by the triple product,

$$g^{(3)}(R_1,R_2,R_{12}) \rightarrow g(R_1)\ g(R_2)\ g(R_{12}) \ . \qquad (15)$$

We have found that calculations of the various distributions of F and G using the superposition approximation agree with the "exact" 2NN results, shown in Figure 1, almost to within the numerical uncertainties of the molecular dynamics results. Moreover, these "2NNS" calculations are orders of magnitude less time consuming that the molecular dynamics computer runs!

Figure 2 shows the mean value and standard deviation of the longitudinal derivative G as a function of the microfield strength. In the 1NN approximation, G is completely correlated with F, and equals 1 in the scaled variables of Figure 2; this is almost always an overestimate of $\bar{G}(F)$. The 2NNS result and the molecular dynamics result are in fairly good agreement at this Γ-value.

3.2 Two-Component Plasmas

The extension of formulae for the one-component plasma to accommodate ionic mixtures is straight forward. For example, the probability that the nearest perturber ion is a type β and is located a distance R from a radiating ion of type α is

$$W_{\alpha\beta}(R)dR = 4\pi\bar{N}_\beta\ g_{\alpha\beta}(R)\ \exp\ [-n_\alpha(R)]\ dR \ , \qquad (16)$$

where now the expected number of ions within a distance R is

$$n_\alpha(R) = 4\pi\int_0^R [\Sigma_\gamma \bar{N}_\gamma\ g_{\alpha\gamma}(s)]\ s^2 ds \ . \qquad (17)$$

The 1NN microfield distribution at a type α ion can be written as

$$P_\alpha(F) = \Sigma_\gamma W_{\alpha\gamma}(R)\ |dR/dF_\gamma| \quad , \tag{18}$$

with $F_\gamma = Z_\gamma e/R^2$. Radial distribution functions $g_{\alpha\beta}(R)$ also are available for mixtures [10], and the 2NNS formulae follow directly from Eq. (15) and Eqs. (16) - (18). Finally, for mixtures the definitions of R_0, Γ, and the normal field F_0 are (cf. [7],[8])

$$\frac{4\pi}{3} R_0^3 \Sigma_\gamma \bar{N}_\gamma = 1;\ \Gamma = \frac{\langle Ze\rangle^2}{R_0 kT}\ ;\ F_0 = \frac{\langle Z^{3/2}\rangle^{2/3} e}{R_0^2} \quad . \tag{19}$$

Analogously to Figure 1, in Figure 3 we have plotted microfield distributions for two cases of high-Z radiators ($Z_r = 5$ and $Z_r = 10$) in a predominantly hydrogen plasma. In these situations, the 1NN approximation seriously underestimates P(F) in the region of interest beyond the peak. The 2NN results are considerably better, but their accuracy here is less than it is for the one-component plasma.

4. Profiles of Isolated Lines

In order to demonstrate the non-linear Stark broadening effects, we computed resonance line ($2^1P - 1^1S$) profiles for Ne^{+8} and Ar^{+16} ions. The neon and argon plasma parameters, adopted from recent diagnostic experiments at U. Rochester [11,12], are listed in Table 1. Except for Λ_D, the number of electrons in a Debye sphere, all quantities have been defined in the text or are self-evident. Also listed are relevant line shape data. Impact widths δ_e were computed from formulae in Sobel'man [13]; in both cases, the impact shift $d \ll \delta_e$, and therefore it was ignored in these illustrative calculations.

Figure 4 shows the profiles ψ_V and ψ_{QS} and their convolution ψ_C for the M = 1 component of each resonance line. The resultant HWHM are considerably larger than those of the Voigt profiles. In consequence, the peak value of ψ_C - to which laser gain is proportional - is much reduced, and so short-wavelength laser schemes involving non-hydrogenic systems (see, eg. [2]) may need reexamination.

An estimate of the relative importance of the ion-quadrupole term can be obtained by comparing profiles for M = 0 and M = 1 components of the same line, since these differ only in the coefficient of G (cf. Eq. 7). This is done in Figure 5 for the Ar^{+16} ($2^1P - 1^1S$) transition, and it is evident that the quadratic-Stark term is much more important in this instance. Our findings, therefore, are in contrast to the work of Lee, et. al. [14], who considered only the ion-quadrupole term in their investigation of non-linear Stark broadening of He-like ion lines in dense plasmas. However, for radiating ions with still higher values of Z_r, the energy denominator in the second-order term $E^{(2)}$ can be much larger, making the ion quadrupole and quadratic-Stark effects comparable.

ACKNOWLEDGMENT

This work was performed under the auspices of the U.S. Department of Energy, and supported by contracts DE-AC02-76-CHO3037 and W-7405-ENG-48.

Table 1. Plasma and Atomic Parameters

Quantity	Neon	Argon
kT (eV)	300	800
$N_e(cm^{-3})$	$7x10^{22}$	$9.6x10^{23}$
$\langle Z \rangle$	9.00	16.8
$\langle Z^2 \rangle$	82.0	280.0
R_0(Bohr)	5.92	3.04
Γ	1.24	3.16
Λ_D	1.04	0.533
$h\nu(^{o}_{ij})$ (eV)	922.0	3139.3
δ_D(eV)	0.165	0.400
δ_e(eV)	0.270	0.497

REFERENCES

1. Bekefi, G., Deutsch, C., and Yaakobi, B.: "Spectroscopic Diagnostics of Laser Plasmas," in Principles of Laser Plasmas, ed. G. Bekefi, J. Wiley and Sons, New York, 1976.

2. McCorkle, R.A., and Joyce, J.M., Phys. Rev. A10, 903 - (1974) 12.

3. Armstrong, B.H.J., Quant. Spectrosc. Radiat. Transfer 7, (1967) 61-88.

4. Griem, H.R., Spectral Line Broadening By Plasmas. Academic Press, New York; § II.3f (1974).

5. Hansen, J.P., and McDonald, I.R., Phys. Rev. Lett. 41, (1978) 1379-82.

6. Hansen, J.P., McDonald, I.R., and Pollock, E.L., Phys. Rev. A11 (1975) 1025-39.

7. Chandrasekhar, S., and von Neumann, J., Astrophys J. 95, (1942) 489-510

8. DeWitt, H.E., Graboske, H.C., and Cooper, M.S., Astrophys. J. 181 (1973) 439-56

9. Alastuey, A., and Jancovici, B., Astrophys. J. 226, (1978) 1034-40.

10. Itoh, N., Totsuji, H., Ichimaru, S. and DeWitt, H.E., Astrophys. J. 234 (1979) 1079-84.

11. Yaakobi, B., Steel, D., Thorsos, E., Hauer, A., Perry, B., Skupsky, S., Geiger, J., Lee, C.M., Letzring, S., Rizzo, J., Mukaiyama, T., Lazarus, E., Halpern, G., Deckman, H., Delettrez, J., Soures, J., and McCrory, R., Phys. Rev. A19 (1979) 1247-62.

12. Yaakobi, B., Skupsky, S., McCrory, R.L., Hooper, C.F., Deckman, H., Bourke, P., and Soures, J.M., Phys. Rev. Lett. 44 (1980) 1072-5.

13. Sobel'man, I.I., Introduction to the Theory of Atomic Spectra. Pergamon Press, Oxford; §39 (1972).

14. Lee, R.W., Bromage, G.E., and Richards, A.G., J. Phys. B12 (1979) 3445-53; and private communication.

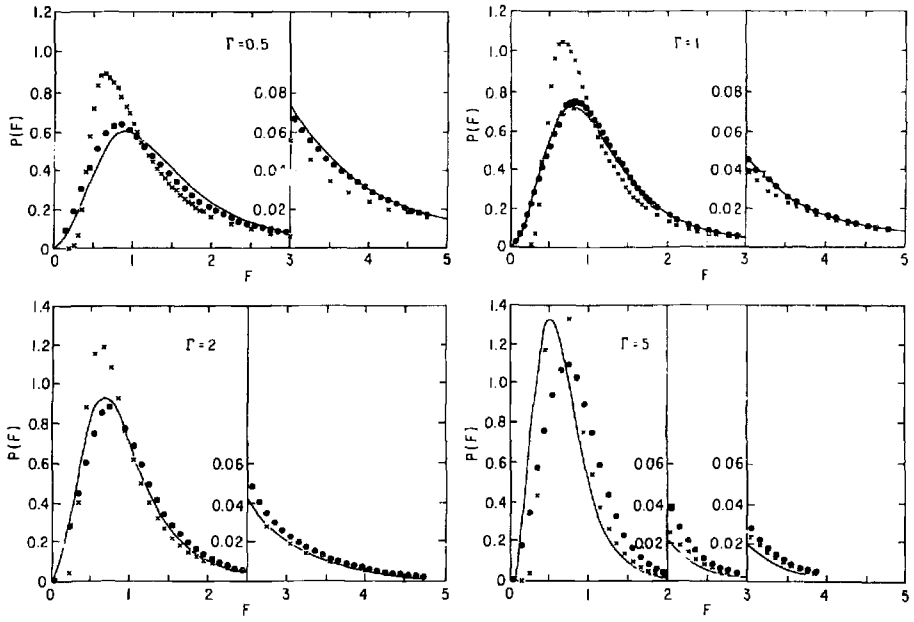

(PPPL-802195)

Fig. 1. Microfield distributions P(F) in one-component plasmas with different Γ values. The unit of field strength is $F_o = Ze/R_0^2$. A solid curve denotes the distribution due to all ions; × denotes the 1NN distribution; ▪ denotes the 2NN distribution.

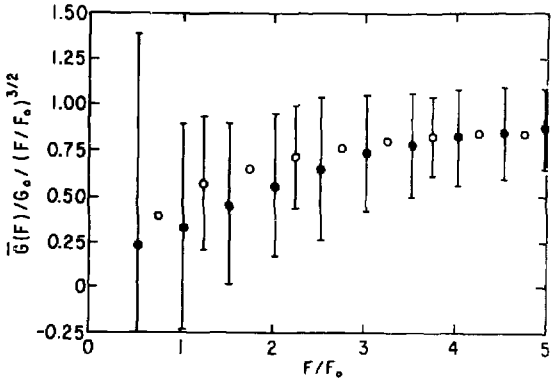

Fig. 2. Conditional mean and standard deviation of the quantity $[G(F)/G_o]/[F/F_o]^{3/2}$, where $F_o = Ze/R_o^2$ and $G_o = Ze/R_o^3$, in a one-component plasma with $\Gamma = 1$. Mean values from the molecular dynamics calculations are denoted by filled circles, while those from the 2NNS approximation are denoted by open circles. Standard deviations are indicated by error bars.

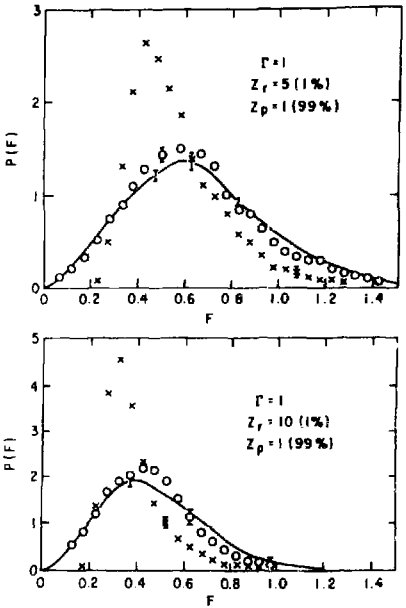

Fig. 3. As in Fig. 1, for $Z_r = 5$ and $Z_r = 10$ in hydrogen plasmas with $\Gamma = 1$.

(PPPL-802196)

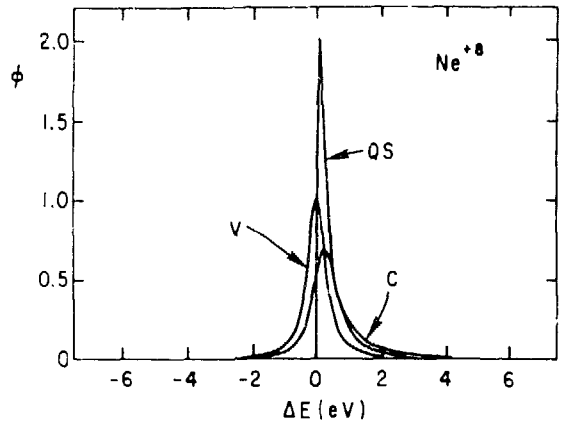

Fig. 4. Voigt (V), quasi-static (QS), and complete (C = <V*QS>) profiles of Ne^{+8} and Ar^{+16} resonance-line components M = 1, for the parameters of Table 1. The unit of all profile functions is $(eV)^{-1}$.

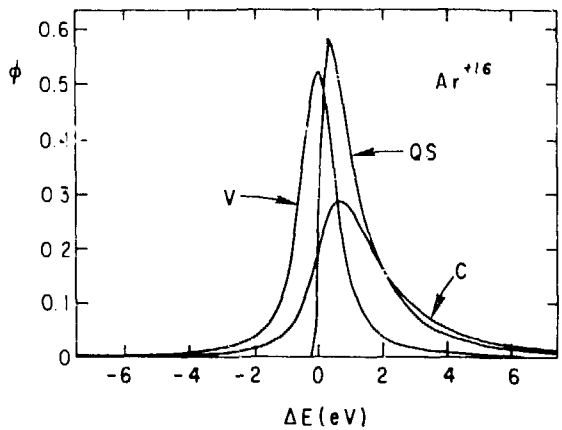

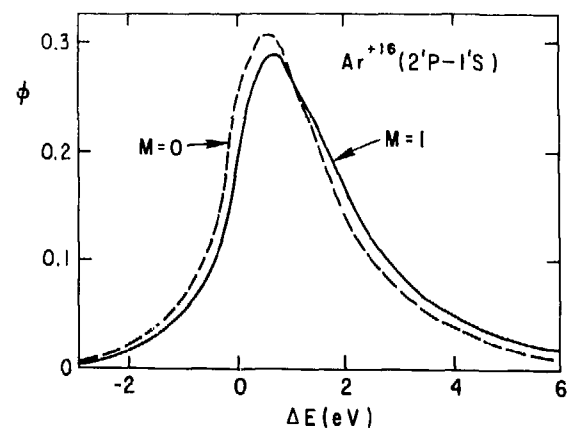

Fig. 5. The complete profile $\phi_C(eV^{-1})$ of the Ar^{+16} resonance-line components M = 0 and M = 1, for the parameters of Table 1.

(PPPL-802194)